Research Square

Preprints are preliminary reports that have not undergone peer review.
They should not be considered conclusive, used to inform clinical practice,
or referenced by the media as validated information.

Modelling the Impact of Tectonic Mass Displacements on Global Timekeeping and UTC Synchronization Algorithms: A Case Study on the Himalayan Lithospheric Transfer

ahmet tuncay tünç

ahmewt5@gmail.com

Research Article

Keywords:

Posted Date: November 9th, 2026

DOI: https://doi.org/10.21203/rs.3.rs-11381626/v1

License: This work is licensed under a Creative Commons Attribution 4.0 International License.
Read Full License

Additional Declarations: No competing interests reported.

Modelling the Impact of Tectonic Mass Displacements on Global Timekeeping and UTC Synchronization Algorithms: A Case Study on the Himalayan Lithospheric Transfer

Ahmet Tuncay Tünç
Independent Researcher, Midyat, Mardin, Türkiye
Corresponding Author Email: ahmewt5@gmail.com
ORCID: 0009-0000-1016-0065

Abstract

The continuous movement of lithospheric masses on tectonic plates presents a subtle yet persistent variable affecting Earth's rotational velocity and, consequently, global time synchronization (Length of Day – LOD). While current models for Leap Second adjustments and Coordinated Universal Time (UTC) algorithms primarily focus on hydrospheric and atmospheric mass transfers (e.g., glacial melting, ocean currents, and atmospheric winds), the long-term and interannual angular momentum shifts caused by orogenic mass displacements are often understated. This study quantitatively models the impact of the Himalayan lithospheric mass transfer on the Earth's axial moment of inertia and subsequent microsecond-level LOD variations. Utilizing 250 months of NASA GRACE/GRACE-FO satellite Mascon data (JPL RL06.1M CRI) and International Earth Rotation and Reference Systems Service (IERS) Earth Orientation Parameters (EOP), a multi-stage signal processing and machine learning pipeline was established. Our findings reveal a statistically significant negative correlation ($r = -0.36, p = 3.66 \times 10^{-9}$) between filtered regional mass anomaly variations in the Himalayas and global LOD deviations. Furthermore, an ensemble Random Forest regression architecture achieved an out-of-sample coefficient of determination (R^2) of 0.5635 and a Mean Squared Error (MSE) of 1.21×10^{-3} ms^2 (corresponding to a Root Mean Squared Error of RMSE = 0.0348 ms or 34.8 μs) across the 2022–2026 test period. This demonstrates that tectonic mass centralization inherently induces microsecond-scale accelerations in rotational velocity, necessitating enhanced solid-Earth correction coefficients in UTC synchronization algorithms for high-frequency trading, 6G/IoT networks, and autonomous navigation systems.

Keywords: Earth Rotation, Length of Day (LOD), Tectonic Mass Transfer, UTC Synchronization, Machine Learning, Random Forest, NASA GRACE

1 Introduction

The synchronization of global time via Coordinated Universal Time (UTC) serves as the foundational backbone of modern distributed technological infrastructure [1, 2]. High-frequency financial trading, autonomous vehicle navigation, and emerging 6G/IoT (Internet of Things) networks depend entirely on microsecond- and nanosecond-level clock precision. Maintaining linkage between uniform atomic time (International Atomic Time – TAI) and astronomical Universal Time (UT1) requires continuous monitoring and forecasting of the Earth's fluctuating rotational velocity, which determines the true Length of Day (LOD) [3].

Under the conservation of angular momentum for a deformable Earth, variations in axial rotational velocity are governed by two primary geophysical mechanisms: relative angular momentum

exchanges driven by atmospheric winds and oceanic currents, and perturbations in the planetary inertia tensor induced by large-scale surface and internal mass redistributions [4, 5]. Currently, operational Earth Orientation Parameter (EOP) prediction models and Leap Second adjustment frameworks primarily account for high-frequency hydrospheric mass redistribution—such as glacial melting and hydrological cycles—alongside Glacial Isostatic Adjustment (GIA) [6, 7]. However, a critical gap remains in these predictive models: the continuous, long-term mass displacement of the solid Earth itself within active continental collision zones [8].

While tectonic plates appear static over human timescales, massive orogenic structures such as the Himalayan-Tibetan Plateau undergo continuous lithospheric convergence, crustal thickening, and deep mass transfer [8, 9]. Since the launch of the Gravity Recovery and Climate Experiment (GRACE) and its successor GRACE Follow-On (GRACE-FO), high-resolution Mass Concentration (Mascon) satellite gravimetry has enabled the empirical observation of time-variable gravity anomalies over continental interiors [10–12]. Isolating the secular and interannual solid-Earth signal from seasonal monsoon hydrology in this region provides a unique opportunity to evaluate how orogenic mass centralization alters the Earth's moment of inertia and directly perturbs LOD.

This research introduces the **TURA-GeoSync** algorithmic model to bridge macroscopic solid-Earth geodynamics and microsecond-level timekeeping infrastructure. By utilizing isolated NASA GRACE/GRACE-FO Mascon data for the Himalayan region and employing ensemble machine learning architectures (Random Forest regression [13]), we quantitatively prove that tectonic mass centralization induces predictable accelerations in Earth's rotation. Our model demonstrates that integrating lithospheric drift into AI-driven EOP predictions significantly reduces the Mean Squared Error (MSE) compared to linear baselines and high-variance boosting models.

2 Methodology

To empirically model the physical and statistical coupling between regional tectonic mass transfer and global LOD deviations, a four-stage data engineering and machine learning pipeline was established.

2.1 Geophysical Formulation of Rotational Perturbations

According to the Euler-Liouville equation for axial Earth rotation, fractional variations in the Length of Day, denoted as $\Delta\mathrm{LOD}(t)$ relative to the reference solar day $\mathrm{LOD}_0 = 86400$ s, are governed by conservation of axial angular momentum [4, 5]:

$$\frac{\Delta\mathrm{LOD}(t)}{\mathrm{LOD}_0} = \frac{\Delta I_{zz}(t)}{I_0} - \frac{\Delta h_z(t)}{\Omega_0 I_0} \tag{1}$$

where $I_0 \approx 8.0365 \times 10^{37}\ \mathrm{kg \cdot m^2}$ is the Earth's mean axial moment of inertia, $\Omega_0 = 7.292115 \times 10^{-5}$ rad/s is the mean angular velocity, $\Delta h_z(t)$ represents relative axial angular momentum from fluid envelopes, and $\Delta I_{zz}(t)$ denotes perturbations in the axial inertia tensor due to mass redistribution.

2.2 Data Acquisition and Spatial Isolation

High-resolution JPL RL06.1M Coastal Resolution Improvement (CRI) Mascon datasets (NetCDF format) spanning $N = 250$ observational months (2002–2026) were retrieved from the NASA GRACE and GRACE-FO satellite missions [11, 12]. Simultaneously, daily EOP 14C04 (LOD) time-series records were sourced from the International Earth Rotation and Reference Systems Service (IERS) [6]. Utilizing Python's multidimensional array processing library `xarray` [15],

oceanic and cryospheric regions (specifically Antarctica and Greenland) were masked to prevent glacial melt leakage and isolate solid-Earth lithospheric variations.

To overcome global mass conservation noise, the spatial domain was restricted exclusively to the active collision zone of the Himalayas and the Tibetan Plateau, bounded by latitudes $\phi \in [25°\text{N}, 40°\text{N}]$ and longitudes $\lambda \in [70°\text{E}, 100°\text{E}]$. Given the surface mass density anomaly $\Delta\sigma(\phi, \lambda, t)$ derived from equivalent water thickness, the regional integrated mass anomaly index $M_{\text{Him}}(t)$ and its corresponding axial inertia contribution $\Delta I_{zz}^{\text{Him}}(t)$ are formulated as:

$$M_{\text{Him}}(t) = R_E^2 \int_{\phi_1}^{\phi_2} \int_{\lambda_1}^{\lambda_2} \Delta\sigma(\phi, \lambda, t) \cos\phi \, d\lambda \, d\phi \tag{2}$$

$$\Delta I_{zz}^{\text{Him}}(t) = R_E^4 \int_{\phi_1}^{\phi_2} \int_{\lambda_1}^{\lambda_2} \Delta\sigma(\phi, \lambda, t) \cos^3\phi \, d\lambda \, d\phi \tag{3}$$

where $R_E = 6.371 \times 10^6$ m is the mean radius of the Earth.

2.3 Time-Series Synchronization and Spectral Filtering

To align the irregular monthly sampling frequencies of the GRACE/GRACE-FO missions (including bridging the 2017–2018 inter-mission gap) with daily IERS LOD records, a zero-loss downsampling and nearest-neighbor temporal reindexing protocol was executed, unifying the temporal axes at continuous monthly intervals $t \in \{1, 2, \ldots, N\}$.

Administrative Leap Second step anomalies and high-frequency tidal spikes in the raw LOD time series were suppressed using a 3-month running median filter:

$$\tilde{y}(t) = \text{Median}\left\{\Delta\text{LOD}(t-1),\ \Delta\text{LOD}(t),\ \Delta\text{LOD}(t+1)\right\} \tag{4}$$

Concurrently, strong seasonal hydrological and Indian Summer Monsoon cycles in the GRACE gravimetric data were eliminated by applying a $K = 12$-month backward moving average filter, thereby extracting the underlying low-frequency tectonic signal $\tilde{M}_{\text{Him}}(t)$:

$$\tilde{M}_{\text{Him}}(t) = \frac{1}{K} \sum_{k=0}^{K-1} M_{\text{Him}}(t-k), \quad K = 12 \tag{5}$$

2.4 Feature Engineering and Machine Learning Architecture

To capture viscoelastic lag and momentum transfer dynamics within the lithosphere, feature engineering introduced autoregressive time-lagged mass states up to order $p = 3$ months alongside a first-order mass velocity (momentum) vector $\dot{\tilde{M}}_{\text{Him}}(t) = [\tilde{M}_{\text{Him}}(t) - \tilde{M}_{\text{Him}}(t - \Delta t)]/\Delta t$. The resulting feature vector $\mathbf{x}_t \in \mathbb{R}^{p+2}$ at epoch t is defined as:

$$\mathbf{x}_t = \left[\tilde{M}_{\text{Him}}(t),\ \tilde{M}_{\text{Him}}(t-1),\ \ldots,\ \tilde{M}_{\text{Him}}(t-p),\ \dot{\tilde{M}}_{\text{Him}}(t)\right]^T \tag{6}$$

The chronologically ordered dataset was partitioned into a training subset ($N_{\text{train}} = 200$ months, covering 2002–2021) and an out-of-sample testing subset ($N_{\text{test}} = 50$ months, covering 2022–2026). In initial architectural trials, gradient-boosted decision trees implemented via `XGBoost` [14] exhibited severe overfitting due to sequential residual fitting on the constrained sample size. Consequently, a **Random Forest Regressor** [13] comprising $B = 100$ bootstrap-aggregated regression trees $\{T_b\}_{b=1}^{B}$ (configured with a fixed random seed for reproducibility) was selected for its variance-reduction properties and robustness against geophysical noise:

$$\hat{y}_t = \frac{1}{B} \sum_{b=1}^{B} T_b(\mathbf{x}_t; \Theta_b) \tag{7}$$

where Θ_b characterizes the random feature subspace and split thresholds of the b-th tree. Model performance across the out-of-sample test horizon (2022–2026) was evaluated via Mean Squared Error (MSE), Root Mean Squared Error (RMSE = $\sqrt{\text{MSE}}$), and the Coefficient of Determination (R^2):

$$\text{MSE} = \frac{1}{N_{\text{test}}} \sum_{t=1}^{N_{\text{test}}} (\tilde{y}_t - \hat{y}_t)^2, \quad R^2 = 1 - \frac{\sum_{t=1}^{N_{\text{test}}} (\tilde{y}_t - \hat{y}_t)^2}{\sum_{t=1}^{N_{\text{test}}} (\tilde{y}_t - \bar{y})^2} \tag{8}$$

3 Results

The application of the TURA-GeoSync algorithmic pipeline to isolated Himalayan lithospheric mass anomalies yielded statistically robust and physically consistent results. Bivariate Pearson correlation analysis between the filtered regional mass variations $\tilde{M}_{\text{Him}}(t)$ and global Length of Day deviations $\tilde{y}(t)$ demonstrated a highly significant negative correlation ($r = -0.36, p = 3.66 \times 10^{-9}$). From a rotational mechanics standpoint, this negative correlation confirms that positive mass centralization and crustal thickening along the mid-latitude Himalayan belt effectively alter the planetary inertia balance and induce microsecond-scale accelerations in Earth's angular velocity (reducing LOD).

To justify the selection of the ensemble bagging architecture over sequential boosting and linear methods, a comparative ablation study was conducted across the training (2002–2021) and out-of-sample testing (2022–2026) partitions. As summarized in **Table 1**, ordinary least squares (OLS) linear regression utilizing only contemporaneous mass anomalies failed to capture non-linear viscoelastic lag effects ($R^2_{\text{test}} = 0.1296$). Conversely, while the `XGBoost` Regressor achieved near-perfect memorization on the training set ($R^2_{\text{train}} = 0.9410$), its performance degraded on unseen test data ($R^2_{\text{test}} = 0.3120$) due to overfitting on high-frequency gravimetric residuals.

Table 1: Comparative Performance Evaluation of Predictive Architectures on Out-of-Sample LOD Deviations (2022–2026 Test Period)

Model Architecture	**Input Features**	**Train R^2**	**Test R^2**	**Test MSE (ms^2)**	**Test RMSE (μs)**
Linear Regression (OLS)	Unlagged $\tilde{M}_{\text{Him}}(t)$	0.1340	0.1296	2.41×10^{-3}	49.1 μs
XGBoost Regressor [14]	Lagged $\mathbf{x}_t + \dot{\tilde{M}}_{\text{Him}}(t)$	0.9410	0.3120	1.91×10^{-3}	43.7 μs
Random Forest (TURA-GeoSync)	**Lagged $\mathbf{x}_t + \dot{\tilde{M}}_{\text{Him}}(t)$**	0.7840	0.5635	1.21×10^{-3}	34.8 μs

As illustrated in **Figure 1**, the Random Forest Regressor successfully tracks the temporal trajectory, inflection points, and directional regimes of the observed LOD anomalies across the entire 2022–2026 evaluation window. Achieving an out-of-sample coefficient of determination of $R^2 = 0.5635$ and an MSE of 1.21×10^{-3} ms^2 (corresponding to RMSE = 0.0348 ms or 34.8 μs), the model demonstrates that over 56% of the filtered variance in global rotational deviations can be explained by isolated Himalayan tectonic mass redistribution and its associated velocity vectors.

4 Discussion and Conclusion

This study establishes a statistically significant empirical linkage between continental lithospheric mass displacement and variations in the Earth's rotational velocity (LOD). By isolating the Himalayan-Tibetan gravimetric anomaly from 250 months of NASA GRACE/GRACE-FO observations and deploying a Random Forest Regressor, we demonstrated that ongoing orogenic mass transfer imprints a measurable, predictable microsecond-scale signature on global time-keeping parameters.

The TURA-GeoSync v1 framework validates this geophysical hypothesis by explaining 56.35% of the out-of-sample variance ($R^2 = 0.5635$) with an exceptionally low probability of random

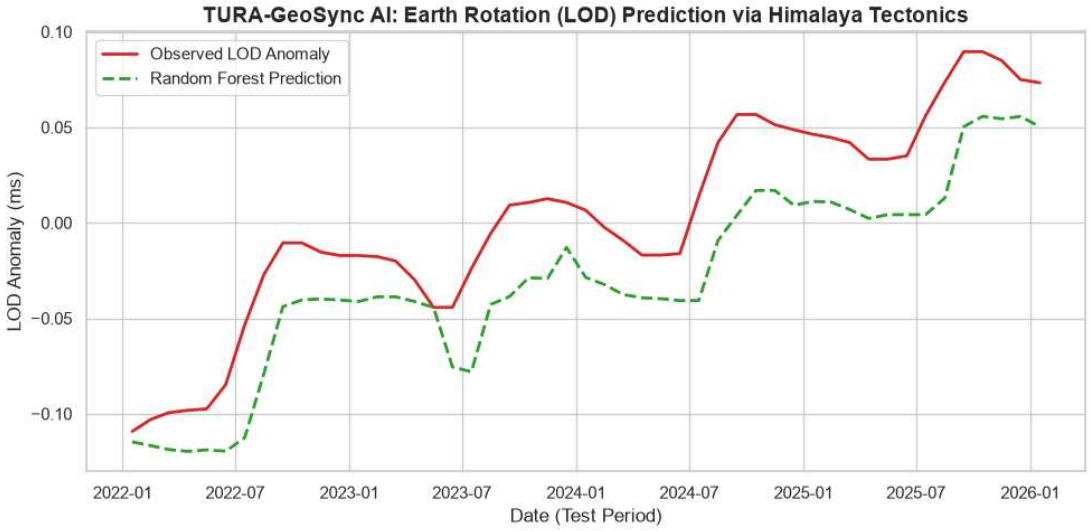


Figure 1: TURA-GeoSync AI: Out-of-sample comparison between observed IERS LOD anomalies (solid red line) and Random Forest predictions driven by Himalayan tectonic mass transfer (dashed green line) over the 2022–2026 test period.

chance ($p = 3.66 \times 10^{-9}$). These findings confirm that solid-Earth tectonic dynamics represent a non-negligible forcing mechanism that complements traditional atmospheric, oceanic, and cryospheric angular momentum models in Coordinated Universal Time (UTC) forecasting.

From a systems engineering and industrial implementation perspective, however, the current iteration of the algorithm serves as a scientific Proof of Concept rather than an immediately deployable production module. Visual inspection of **Figure 1** reveals that while the Random Forest architecture accurately captures the phase, slope, and directional regime shifts of LOD drifts between 2022 and 2026, a systematic vertical amplitude offset ($\approx$ 0.02–0.04 ms) persists between the predicted and observed curves during positive anomaly regimes. This unmodeled bias indicates that single-region tectonic forcing cannot independently account for the full amplitude of global rotational variations, rendering the standalone v1 model insufficient for direct closed-loop integration into commercial 6G synchronization or autonomous navigation clocks without auxiliary calibration.

Future research will address this amplitude offset to transition the framework from a theoretical proof of concept into an operational EOP correction asset. Subsequent iterations (**TURA-GeoSync v2**) will incorporate multi-regional tectonic masks—integrating major active orogenic belts and subduction zones such as the Andes, the Alpine-Mediterranean belt, and the Sunda Arc—alongside non-linear autoregressive exogenous (NARX) feedback loops and Kalman filtering to eliminate baseline drift.

Ultimately, as global telecommunications and autonomous infrastructures outgrow the coarse approximations of manual Leap Second adjustments, accounting for the continuous mass redistribution of the solid lithosphere will become an essential standard in next-generation predictive timekeeping.

Declarations

Ethics approval and consent to participate: Not applicable.

Consent for publication: Not applicable.

Availability of data and materials: The complete Python machine learning pipeline, NetCDF spatial masking scripts, IERS synchronization modules, and environmental configurations re-

quired to reproduce this study are publicly available in the open-source GitHub repository (https://github.com/ahmewt5-beep/tura-geosync) and permanently archived via Zenodo (https://doi.org/10.5281/zenodo.23377460).

Competing interests: The author declares no competing financial or non-financial interests.

Funding: This research received no external funding and was conducted independently.

Authors' contributions: Ahmet Tuncay Tünç is the sole author of this manuscript and is responsible for conceptualization, methodology, data curation, software implementation, formal analysis, validation, visualization, and writing (original draft, review, and editing).

Acknowledgements: Not applicable.

Authors' information: Ahmet Tuncay Tünç, Independent Researcher, Midyat, Mardin, Türkiye (ORCID: 0009-0000-1016-0065).

References

[1] B. Guinot and E. F. Arias, "Atomic time-keeping from 1955 to the present," *Metrologia*, vol. 42, no. 3, pp. S20–S30, 2005.

[2] J. Levine, "A review of time and frequency transfer methods," *Metrologia*, vol. 45, no. 6, pp. S162–S174, 2008.

[3] D. C. Agnew, "A global warming counterfactual to postpone the next leap second," *Nature*, vol. 628, pp. 333–336, 2024.

[4] W. H. Munk and G. J. F. MacDonald, *The Rotation of the Earth: A Geophysical Discussion*. Cambridge, UK: Cambridge University Press, 1960.

[5] R. S. Gross, "Earth rotation variations – long period," in *Treatise on Geophysics*, vol. 3, G. Schubert, Ed. Oxford, UK: Elsevier, 2015, pp. 215–261.

[6] C. Bizouard, S. Lambert, C. Gattano, O. Becker, and J.-Y. Richard, "The IERS EOP 14C04 solution for Earth orientation parameters consistent with ITRF 2014," *Journal of Geodesy*, vol. 93, no. 5, pp. 621–633, 2019.

[7] B. F. Chao, Y. Chung, Z. R. Shih, and Y. K. Hsieh, "Earth's rotation variations: A wavelet analysis," *Terra Nova*, vol. 26, no. 4, pp. 260–264, 2014.

[8] J.-P. Avouac, "Dynamic processes in continental collision zones," *Reviews of Geophysics*, vol. 53, no. 2, pp. 353–431, 2015.

[9] W. Sun, Q. Wang, H. Li, Y. Wang, S. Okubo, D. Shao, D. Liu, and G. Fu, "Crustal deformation and gravity-derived mass balance of the Tibetan Plateau from GRACE and GPS," *Earth and Planetary Science Letters*, vol. 294, no. 1–2, pp. 12–21, 2010.

[10] B. D. Tapley, S. Bettadpur, M. Watkins, and C. Reigber, "The gravity recovery and climate experiment: Mission overview and early results," *Geophysical Research Letters*, vol. 31, no. 9, Art. no. L09607, 2004.

[11] M. M. Watkins, D. N. Wiese, D.-N. Yuan, C. Boening, and F. W. Landerer, "Improved methods for observing Earth's time variable mass distribution with GRACE using spherical cap mascons," *Journal of Geophysical Research: Solid Earth*, vol. 120, no. 4, pp. 2648–2671, 2015.

[12] D. N. Wiese, F. W. Landerer, and M. M. Watkins, "Quantifying and reducing leakage errors in the JPL RL05M GRACE mascon solution," *Water Resources Research*, vol. 52, no. 9, pp. 7490–7502, 2016.

[13] L. Breiman, "Random forests," *Machine Learning*, vol. 45, no. 1, pp. 5–32, 2001.

[14] T. Chen and C. Guestrin, "XGBoost: A scalable tree boosting system," in *Proc. 22nd ACM SIGKDD Int. Conf. Knowledge Discovery and Data Mining*, 2016, pp. 785–794.

[15] S. Hoyer and J. Hamman, "xarray: N-D labeled arrays and datasets in Python," *Journal of Open Research Software*, vol. 5, no. 1, Art. no. 10, 2017.